ACS Energy LETTERS

http://pubs.acs.org/journal/aelccp

High Energy Density Aqueous Flow Battery Utilizing Extremely Stable, Branching-Induced High-Solubility Anthraquinone near Neutral pH

Emily F. Kerr,[#] Zhijiang Tang,[#] Thomas Y. George, Shijian Jin, Eric M. Fell, Kiana Amini, Yan Jing, Min Wu, Roy G. Gordon,[*] and Michael J. Aziz[*]

Cite This: *ACS Energy Lett.* 2023, 8, 600−607

Read Online

ACCESS | Metrics & More | Article Recommendations | Supporting Information

ABSTRACT: An anthraquinone featuring a chiral carboxylate-capped methyl-branched side chain with an ether linkage, 2,2′-((9,10-dioxo-9,10-dihydroanthracene-2,6-diyl)bis(oxy))-dipropionic acid (2,6-D2PEAQ), was synthesized and evaluated for use in aqueous redox flow batteries. It was found to have an extraordinary solubility of 2 M (4 M electrons), corresponding to a theoretical volumetric capacity of 107.2 Ah/L for the negative electrolyte, which is 10 times that of its unbranched counterpart. The 2,6-D2PEAQ molecule demonstrated stability against thermal decomposition and was extremely stable under cell cycling conditions. A capacity fade rate of 0.02%/day over 14 days was demonstrated in a 1.1 M 2,6-D2PEAQ nearly capacity-balanced cell when paired with a ferro-/ferricyanide posolyte at pH 7. Compared to other aqueous redox-active organic molecules, its demonstrated fade rate is lower than that of any molecule with a demonstrated volumetric capacity of ≥55 Ah/L, and its volumetric capacity is greater than that of any molecule with a demonstrated fade rate of ≤0.5%/day.

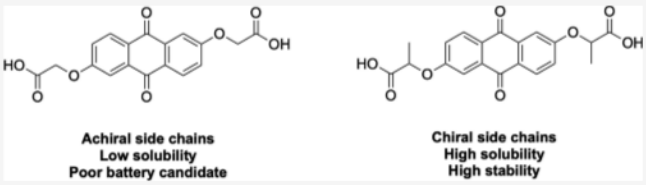

As solar and wind energy installations become more prevalent, there will be an increased opportunity for affordable and scalable energy storage technologies to manage the inherent intermittency of these energy sources and to help manage peak shaving and load leveling for the electrical grid.[1−4] Because redox flow batteries (RFBs) decouple power and energy capacity in the battery, great engineering flexibility is available to design them for grid-level applications.[5−7]

Whereas a variety of different electroactive materials have been tested in redox flow batteries, vanadium is a popular electroactive material because of its four accessible redox states.[8−10] However, vanadium suffers from volatile prices.[11] Organic molecules can offer tunable physical properties that allow the potential for high solubility, high stability, and potentially low-cost electroactive materials.[12,13] Electroactive organic structures including quinones,[14−33] ferrocenes,[34−38] viologens,[39−42] phenazines,[43−47] alloxazines,[48] and nitroxide radicals[47,49−53] have been explored as potential electrolyte species for aqueous organic redox flow batteries.

Anthraquinone derivatives are attractive negolyte (negative electrolyte) redox active species in aqueous redox flow batteries because of their facile kinetics and low redox potentials. In alkaline conditions, several anthraquinone derivatives exhibit over 0.5 M solubility in aqueous solutions with temporal degradation rates below 0.04%/day in full cell charging/discharging cycling.[12,19,24,25,31] However, previous anthraquinone derivatives have required high pH or specific counterions to exhibit sufficient solubility, which limits the solubility of ferrocyanide, which is the most readily available positive redox molecule for neutral and alkaline conditions.[54−57] While other anthraquinones that can cycle at neutral pH have been reported,[20] fade rates have been high. Here, we present an anthraquinone derivative that achieves high solubility at mild pH with an extremely low fade rate (<0.02%/day)[12] at a potentially low cost.[58]

We designed 2,2′-((9,10-dioxo-9,10-dihydroanthracene-2,6-diyl)bis(oxy))dipropionic acid (abbreviated 2,6-di-2-propionate ether anthraquinone, 2,6-D2PEAQ, Scheme 1, 384.34 g/mol) for a high-capacity high-stability negolyte (^{1}H NMR in Figure S1). This molecule features a branched side chain

Received: July 26, 2022
Accepted: October 26, 2022

https://doi.org/10.1021/acsenergylett.2c01691
ACS Energy Lett. 2023, 8, 600−607

Scheme 1. 2,6-D2PEAQ Synthetic Route: 2,6-D2PEAQ (Shown on Right) Is Synthesized by Alkylation with Methyl 2-Bromopropionate Ester Followed by Hydrolysis to the Carboxylic Acid[a]

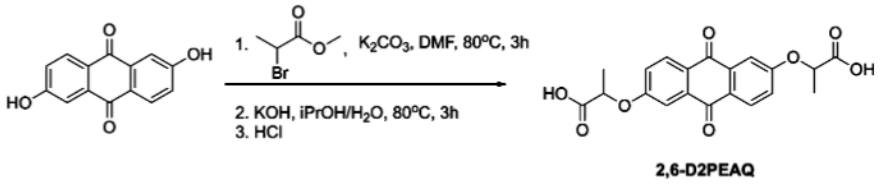

[a]Synthetic details can be found in the Supporting Information.

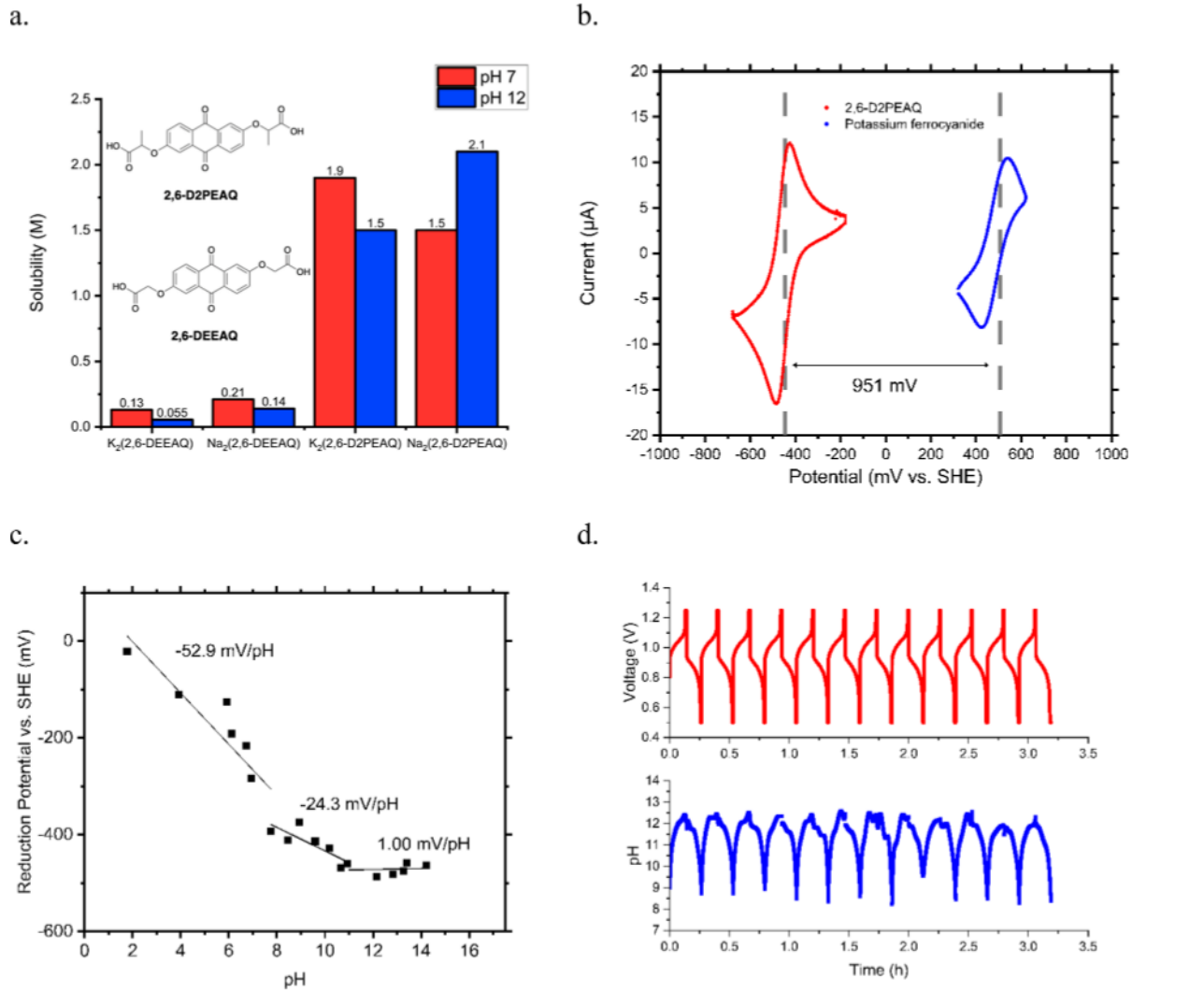

Figure 1. a. Solubility of 2,6-D2PEAQ: High solubility was obtained for 2,6-D2PEAQ at both neutral and alkaline conditions in both potassium and sodium counterions. 2,6-DEEAQ, an analog without a branching methyl, showed poor solubility in similar conditions despite having fewer hydrophobic methyl groups. b. Cyclic voltammogram of 1 mM 2,6-D2PEAQ and 1 mM ferrocyanide at pH 14 in KOH at a scan rate of 0.1 V/s. c. Pourbaix diagrams of 2,6-D2PEAQ. d. First 12 cycles of pH swing cell of a flow battery negolyte containing 0.1 M 2,6-D2PEAQ.

derived from methyl 2-bromopropanoate that is significantly less expensive at lab scales than the side chain derived from ethyl 4-bromobutanoate used in previous work (Supporting Information Table 1).[19]

This branching moiety was designed to slow an S_N2 nucleophilic attack by hydroxide ions by replacing the primary sp^3 carbon adjacent to the ether linkage with a secondary sp^3 hybridized carbon that will experience a slower nucleophilic attack. An intramolecular attack by carboxylate anions has also been previously proposed to cause side chain loss in ether-linked anthraquinones at moderate pH ranges.[19,24] Decomposition by this mechanism would be potentially slowed with the shorter branched side chain because it would require a highly strained 3-member ring transition state to attack at the sp^3 carbon adjacent to the ether oxygen. ^{1}H NMR thermal decomposition studies showed no detectable loss of side chain in either the oxidized or the reduced state when 2,6-D2PEAQ was stored at 90 °C for 1 week at pH 12 (Figures S3−S7).

https://doi.org/10.1021/acsenergylett.2c01691
ACS Energy Lett. 2023, 8, 600−607

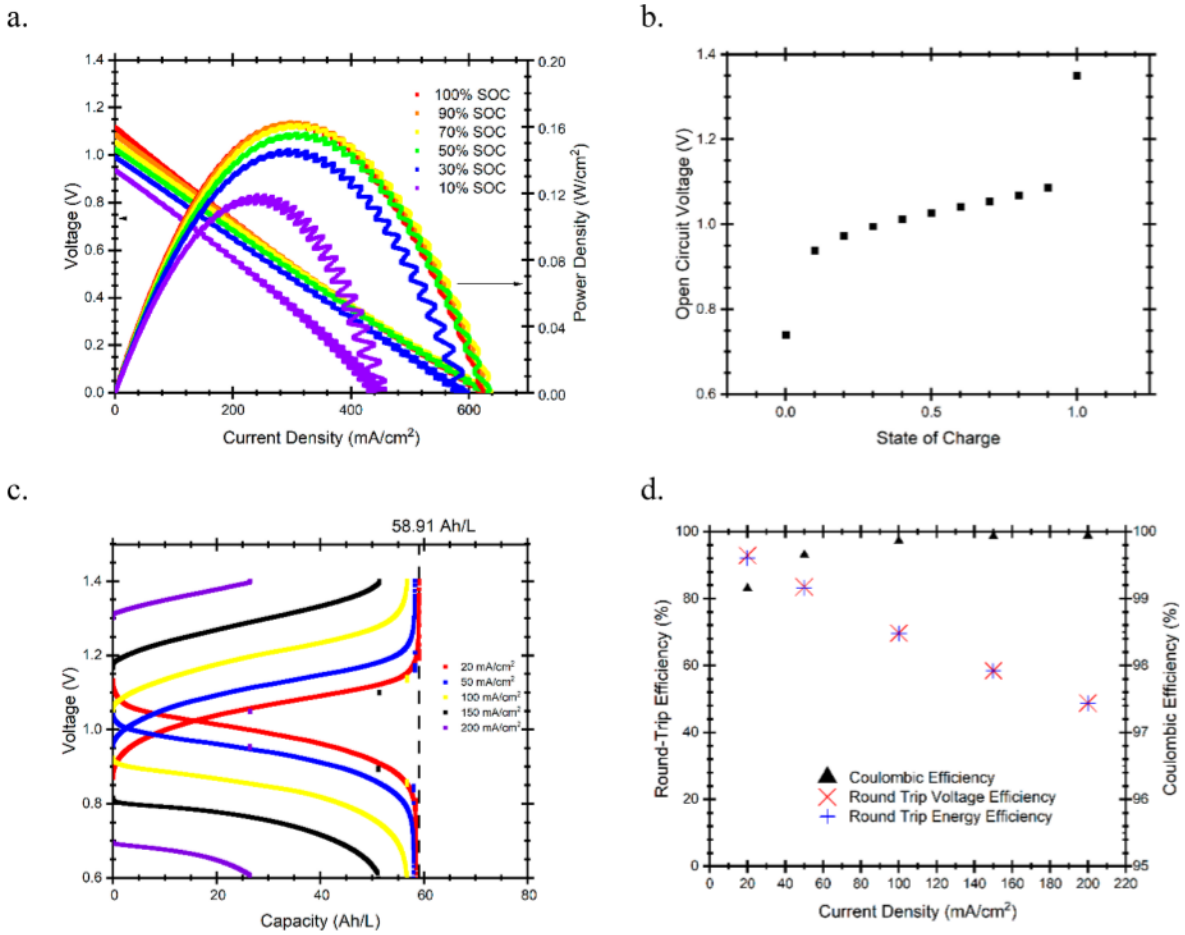

Figure 2. a. High concentration battery comprised a 1.1 M (5.3 mL) 2,6-D2PEAQ capacity-limiting negolyte and 30 mL of 0.6 M sodium ferrocyanide, 0.4 M potassium ferrocyanide, and 0.2 M sodium ferricyanide posolyte at an initial pH of 7. The cell was maintained at 40 °C. b. Cell voltage and power density vs current density at 40 °C at various SOCs. B. OCV vs SOC. c. Charge/discharge voltage profiles at various current densities. The dotted line represents the full theoretical capacity, estimated by Coulomb counting. d. Coulombic, round-trip voltage, and round-trip energy efficiencies at current densities up to 200 mA/cm^2.

This molecule was found to have high solubility. Solubility measurements were obtained by dissolving the maximum possible amount of 2,6-D2PEAQ in an appropriate solution, followed by UV−visible spectrophotometry (Figures 1a, S8−S9). Using potassium hydroxide to deprotonate the carboxylic acid group and then adjusting the pH using HCl, 2,6-D2PEAQ was found to dissolve up to 2.0 M at pH 7 and 2.1 M at pH 12. If sodium hydroxide is used instead of potassium hydroxide, a solubility of 1.9 M at pH 7 and 1.5 M at pH 12 can be achieved. For comparison, a similar anthraquinone, diethanoic ether anthraquinone 2,2′-((9,10-dioxo-9,10-dihydroanthracene-2,6-diyl)bis(oxy))diacetic acid (DEEAQ, 359.29 g/mol, ^{1}H NMR in Figure S2), whose core is joined to the carboxylate solubilizing group by one methylene unit, was synthesized and found to have far lower solubilities. 2,6-DBEAQ (4,4′-((9,10-anthraquinone-2,6-diyl)dioxy)dibutyrate), a previously published molecule with a three-carbon unbranched ether-linked side chain, also did not exhibit the high solubilities of 2,6-D2PEAQ at pH 12 or 14 and did not show any appreciable solubility at neutral pH.[19] This indicates the branching methyl of 2,6-D2PEAQ may play an important role in its high solubility.

This high solubility could be caused by a less energetically favorable crystallization process due to the branch in the side chains, as well as the presence of two enantiomers and one diastereomer due to the chiral carbon caused by the branch on each chain.[59,60] The high solubility of 2,6-D2PEAQ with both potassium and sodium counterions allows a mixed-electrolyte salt to be used in cell cycling, which takes advantage of the increased solubility of ferrocyanide in mixed sodium/potassium cation solutions.[56]

Figure 1b shows cyclic voltammetry of 1 mM 2,6-D2PEAQ in a pH 14 solution of potassium hydroxide. The reduction potential is −445 mV vs SHE with a peak separation of 68 mV at 0.1 V/s, enabling a theoretical cell voltage of 951 mV when paired with a ferrocyanide positive electrolyte (posolyte). Additional CV studies in an unbuffered solution at pH 7 and pH 12 showed a reduction potential of −499 mV vs SHE at pH 12 and −460 mV vs SHE at pH 7 with a peak separation of 56 mV and 53 mV, respectively (Figure S10). Pourbaix diagram analysis (Figure 1c) shows a slope of −53 mV/pH unit from pH 1.8 to pH 7.8, followed by a slope of −24 mV/pH unit from pH 7.8 to pH 10.9, indicating a transition from a $2H^+/2e^-$ process to a $1H^+/2e^-$ process. This is followed by a flat proton-decoupled electron transfer region when the pH is above 10.9 (experimental details in Supporting Information XI). Using rotating disk voltammetry studies, a diffusion coefficient of 2.75×10^{-6} cm^2/s and a rate constant of 3.40×10^{-3} cm s^{-1} were shown (Figure S11).

https://doi.org/10.1021/acsenergylett.2c01691
ACS Energy Lett. 2023, 8, 600−607

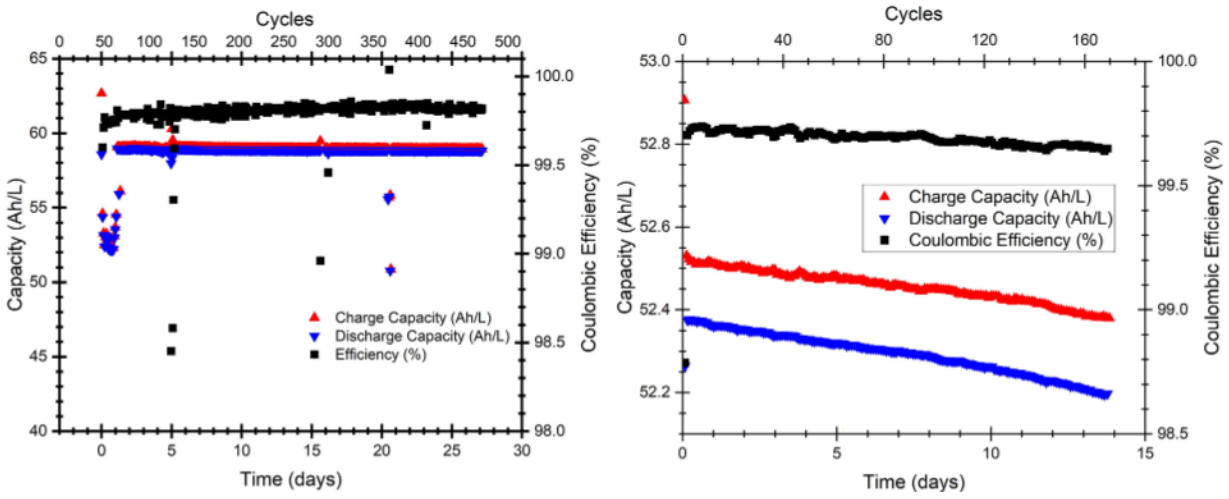

Figure 3. Long-term cycling of both high-concentration and high-concentration nearly balanced cells. Capacities are reported in Ah per liter of negolyte. a. Charge and discharge capacity and Coulombic efficiency for the 1.1 M 2,6-D2PEAQ cell of Figure 2. The dip at day 5 is attributed to a disruption in nitrogen flow to the glovebag. b. Nearly balanced 2,6-D2PEAQ cell at high concentrations, 1.1 M 2,6-D2PEAQ (4.5 mL) and 1.0 M ferrocyanide (14 mL), in which the number of equivalents of ferrocyanide is reduced to 1.4, shows a capacity fade rate of 0.02%/day.

A pH swing cell was prepared in a glovebox at 0.1 M concentration of 2,6-D2PEAQ, 0.1 M potassium ferrocyanide, and 0.04 M potassium ferricyanide. The cell consisted of a normal flow cell with a pH meter installed to measure the pH of the negolyte. The cell cycled reversibly between pH 9 and pH 12 for 22.2 h (Figure 1d). To separate the behavior of 2,6-D2PEAQ from that of the ferrocyanide posolyte, a symmetric cell was separately prepared at 0.1 M 2,6-D2PEAQ and showed a capacity fade rate of 0.04%/day over 4 days when a potential difference square wave with amplitude 200 mV was imposed (Figures S12−S13). pH swing cells have been reported previously to demonstrate pH changes in a cell during cycling.[20,24]

We prepared a flow battery with 0.1 M 2,6-D2PEAQ as the capacity limiting electrolyte that showed a capacity fade rate dependent on the voltage cutoffs (Figure S14).[33,42] A narrow voltage window and, particularly, a lower charging voltage cutoff were shown to slow capacity fade without meaningfully changing capacity utilization. Hence, voltage cutoffs of 0.5 and 1.25 V were chosen for further evaluation. A 0.5 M 2,6-D2PEAQ cell was then tested at 40 °C and showed a capacity fade rate of 0.01%/day (Figure S15). The exact cause of this capacity fade was not studied; however, 2,6-D2PEAQ may share decomposition routes by side chain loss and anthrone formation with other anthraquinones.[19,61,62]

A high concentration battery used a 1.1 M 2,6-D2PEAQ negolyte to test cell performance under realistic concentration conditions (Figure 2a-d). An elevated temperature of 40 °C was chosen to mimic industrial operating conditions. The cell used a potassium form Nafion 212 membrane and an electrode consisting of two layers of SGL 39AA carbon paper in each electrode compartment. To suppress reversible chemical oxidization by atmospheric O_2, the cell was run in a glovebag under a nitrogen atmosphere with constant purge. A pair of cartridge heaters controlled by an Omega CS8DBPT PID controller was used to maintain the temperature. Polarization studies showed a peak power density of 0.16 W/cm^2 at a current density of 300 mA/cm^2 and 100% SOC. The open circuit voltage of this battery was 1.09 V at 90% state of charge (SOC).

This 1.1 M cell was charged and discharged galvanostatically with a current density of 100 mA/cm^2, followed by voltage holds at 1.25 V during charging and 0.5 V during discharging, until the current density dropped below 2 mA/cm^2. The cell was cycled for 27 days (470 cycles). The high-frequency resistance of the cell was 2.35 Ω*cm^2, which refers to the ohmic resistance, contributed mostly by the membrane. The Coulombic efficiency was greater than 99.8%. This cell lost capacity at a rate of 0.013%/day or 0.0008%/cycle between day 7 and day 27 (cycle 119 and cycle 470 (Figure 3a). This is equivalent to 4.7% capacity fade per year. This cell used an excess of posolyte to prevent air oxidation and posolyte decomposition from interfering with accurate monitoring of the capacity change of the negolyte. In combination with the oversupplied posolyte, the electrolytes together exhibit a volumetric capacity of 8.8 Ah/L and an energy density of 8.4 Wh/L. A measured volumetric capacity of 54.6 Ah/L and a theoretical volumetric capacity of 59.0 Ah/L by Coulomb counting for the negolyte alone were realized. The difference is likely due to moisture in the 2,6-D2PEAQ solid. Using a posolyte with balanced capacity, a theoretical energy density of 18.7 Wh/L would be attainable with these concentrations. A negolyte and posolyte at their respective solubility limits would deliver a theoretical volumetric capacity of 20.1 Ah/L and a theoretical energy density of 19.1 Wh/L.

For practical designs, we expect the energy density of the cell to be raised. To explore this prospect, we evaluated a cell containing 4.5 mL of 1.1 M 2,6-D2PEAQ and 14 mL of 1.0 M ferrocyanide, i.e., 1.4 equiv of ferrocyanide, composed of 0.3 M potassium ferrocyanide and 0.7 M sodium ferrocyanide to maximize solubility (Figure 3b). To further increase solubility, 2,6-D2PEAQ was prepared with a 1:1 ratio of sodium to potassium cations (Supporting Information XVI). The concentration was chosen because it maintained high-capacity density without posing engineering challenges associated with the complex rheology observed at higher concentrations. A slight excess of posolyte was used to ensure decomposition of the negolyte was measured and the cell did not go out of balance. This cell had a realized volumetric capacity of 59.0 Ah/L in the negolyte, an energy density of 13.6 Wh/L, and a

https://doi.org/10.1021/acsenergylett.2c01691
ACS Energy Lett. 2023, 8, 600−607

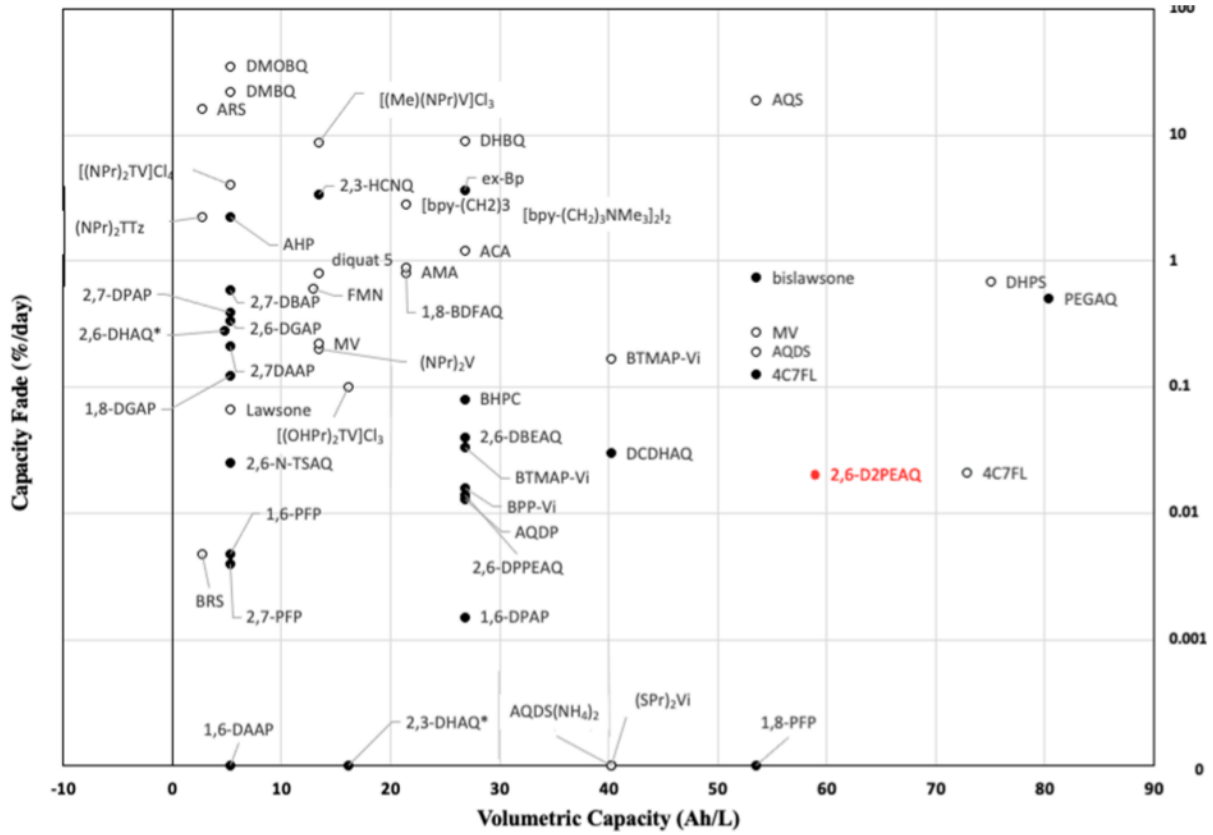

Figure 4. Daily capacity fade vs demonstrated negolyte volumetric capacity of reported aqueous organic flow battery negolytes. Demonstrated capacity fade rates of cells run with potential holds are plotted as filled circles. Apparent capacity fade rates of cells run without potential holds are plotted as hollow circles. Cells that used electrochemical capacity recovery are marked with a star. Data are from refs 16, 19, 20, 22−24, 27, 28, 31−33, 37, 42−46, 48, 62, 64−82.

volumetric capacity of 14.3 Ah/L in the battery overall. This cell was cycled for 14 days and showed a capacity fade rate of 0.02%/day and a Coulombic efficiency of 99.7%.

2,6-D2PEAQ was compared to all other reported aqueous organic negolytes that have been demonstrated to cycle at least 0.1 M electrons for at least 10 cycles in a flow battery. The slowest-fading example of each negolyte is represented in Figure 4 (In cases where the lower demonstrated fade rate had a significantly lower volumetric capacity than another reported cell of the same molecule, both points are plotted.). Temporal fades were estimated from the electrode geometric area and current density where not provided. Where multiple runs of a compound were reported in a single paper, the highest concentration run was plotted. 2,6-D2PEAQ demonstrated the highest energy density of any molecule with a demonstrated fade of less than 0.5%/day. 1,8-PFP, a phenazine, demonstrates improved capacity fade relative to 2,6-D2PEAQ with only slightly lower demonstrated capacity. Note that 4C7FL, a fluorenone derivative, exhibited an apparent capacity fade rate equal to that of 2,6-D2PEAQ when the cell was run galvanostatically but exhibited a higher demonstrated capacity fade rate than 2,6-D2PEAQ when the cell was run with intermittent potential holds to control the effects of changing cell resistance—a testament to the importance of potentiostatic processes, distinguished by the nomenclature of "apparent capacity fade" vs "demonstrated capacity fade".[63]

The cost of the active anthraquinone material might be further lowered by attaching the highly solubilizing side chain to less expensive anthraquinones. 2,6-D2PEAQ analogs starting from 1,8-dihydroxyanthraquinone and 1,4-dihydroxyanthraquinone were synthesized (Figures S16−S17); however, they were found to have unacceptably high capacity fade rates of 2.8%/day and 1.1%/day, respectively (Figures S18 and S19).

In conclusion, 2,6-D2PEAQ, an anthraquinone functionalized with a low-cost chiral side chain, is extremely stable even when cycling at elevated temperatures and high concentrations. The ability to operate at mild pH as the negolyte cycles between pH 9 and pH 12 also reduces the cost of electrolyte-contacting materials and maximizes the solubility of the ferrocyanide posolyte. 2,6-D2PEAQ can dissolve to concentrations up to 2.1 M in both neutral and alkaline pH. This is a dramatic increase in solubility over the analog without a methyl branch. Flow batteries using 2,6-D2PEAQ in the negolyte have demonstrated an extremely low fade rate of ≤0.02%/day or ≤7.3%/year and a realized negolyte volumetric capacity of 58.9 Ah/L. Compared to other aqueous redox-active organic molecules, its demonstrated fade rate is lower than that of any molecule with a demonstrated volumetric capacity of ≥55 Ah/L, and its volumetric capacity is greater than that of any molecule with a demonstrated fade rate of ≤0.5%/day. The use of chiral, branching, and other variations on side chains is a promising direction for further increases in the solubility and stability of redox-active organics.

https://doi.org/10.1021/acsenergylett.2c01691
ACS Energy Lett. 2023, 8, 600−607

■ ASSOCIATED CONTENT

Supporting Information

The Supporting Information is available free of charge at https://pubs.acs.org/doi/10.1021/acsenergylett.2c01691.

Detailed additional synthesis, cell testing, solubility, and stability data (PDF)

■ AUTHOR INFORMATION

Corresponding Authors

Roy G. Gordon − *Department of Chemistry and Chemical Biology, Harvard University, Cambridge, Massachusetts 02138, United States; Harvard John A. Paulson School of Engineering and Applied Sciences, Harvard University, Cambridge, Massachusetts 02138, United States;* orcid.org/0000-0001-5980-268X; Email: gordon@chemistry.harvard.edu

Michael J. Aziz − *Harvard John A. Paulson School of Engineering and Applied Sciences, Harvard University, Cambridge, Massachusetts 02138, United States;* orcid.org/0000-0001-9657-9456; Email: maziz@harvard.edu

Authors

Emily F. Kerr − *Department of Chemistry and Chemical Biology, Harvard University, Cambridge, Massachusetts 02138, United States;* orcid.org/0000-0002-5750-1514

Zhijiang Tang − *Harvard John A. Paulson School of Engineering and Applied Sciences, Harvard University, Cambridge, Massachusetts 02138, United States*

Thomas Y. George − *Harvard John A. Paulson School of Engineering and Applied Sciences, Harvard University, Cambridge, Massachusetts 02138, United States*

Shijian Jin − *Harvard John A. Paulson School of Engineering and Applied Sciences, Harvard University, Cambridge, Massachusetts 02138, United States;* orcid.org/0000-0001-9450-9606

Eric M. Fell − *Harvard John A. Paulson School of Engineering and Applied Sciences, Harvard University, Cambridge, Massachusetts 02138, United States;* orcid.org/0000-0003-2046-1480

Kiana Amini − *Harvard John A. Paulson School of Engineering and Applied Sciences, Harvard University, Cambridge, Massachusetts 02138, United States*

Yan Jing − *Department of Chemistry and Chemical Biology, Harvard University, Cambridge, Massachusetts 02138, United States;* orcid.org/0000-0002-5669-4609

Min Wu − *Harvard John A. Paulson School of Engineering and Applied Sciences, Harvard University, Cambridge, Massachusetts 02138, United States*

Complete contact information is available at: https://pubs.acs.org/10.1021/acsenergylett.2c01691

Author Contributions

#E.F.K. and Z.T. contributed equally.

Notes

The authors declare the following competing financial interest(s): Two of us (R.G.G. and M.J.A.) acknowledge significant financial stakes in Quino Energy, Inc., which might profit from the results reported here.

■ ACKNOWLEDGMENTS

This research was supported by the National Science Foundation through grant CBET-1914543 and by U.S. DOE award DE-AC05-76RL01830 through PNNL subcontract 535264. The authors thank Daniel Pollack for ideas and conversation as well as proofreading assistance. This paper is dedicated to Dr. Zhijiang Tang, a valued and insightful collaborator and scientist. We are deeply saddened by his passing.

■ REFERENCES

(1) Denholm, P.; Ela, E.; Kirby, B.; Milligan, M. *The Role of Energy Storage With Renewable Electricity Generation*; National Renewable Energy Laboratory: 2010; DOI: 10.2172/972169.

(2) Rugolo, J.; Aziz, M. J. Electricity storage for intermittent renewable sources. *Energy Environ. Sci.* **2012**, *5* (5), 7151−7160.

(3) Dunn, B.; Kamath, H.; Tarascon, J. M. Electrical energy storage for the grid: a battery of choices. *Science* **2011**, *334* (6058), 928−35.

(4) Baumann, M.; Peters, J. F.; Weil, M.; Grunwald, A. CO2 Footprint and Life-Cycle Costs of Electrochemical Energy Storage for Stationary Grid Applications. *Energy Technol-Ger* **2017**, *5* (7), 1071−1083.

(5) Soloveichik, G. L. Flow Batteries: Current Status and Trends. *Chem. Rev.* **2015**, *115* (20), 11533−58.

(6) Winsberg, J.; Hagemann, T.; Janoschka, T.; Hager, M. D.; Schubert, U. S. Redox-Flow Batteries: From Metals to Organic Redox-Active Materials. *Angew. Chem., Int. Ed. Engl.* **2017**, *56* (3), 686−711.

(7) Luo, J. A.; Hu, B.; Hu, M. W.; Zhao, Y.; Liu, T. L. Status and Prospects of Organic Redox Flow Batteries toward Sustainable Energy Storage. *ACS Energy Letters* **2019**, *4* (9), 2220−2240.

(8) Noack, J.; Roznyatovskaya, N.; Herr, T.; Fischer, P. The Chemistry of Redox-Flow Batteries. *Angew. Chem., Int. Ed. Engl.* **2015**, *54* (34), 9776−809.

(9) Darling, R. M.; Gallagher, K. G.; Kowalski, J. A.; Ha, S.; Brushett, F. R. Pathways to low-cost electrochemical energy storage: a comparison of aqueous and nonaqueous flow batteries. *Energy Environ. Sci.* **2014**, *7* (11), 3459−3477.

(10) Li, L. Y.; Kim, S.; Wang, W.; Vijayakumar, M.; Nie, Z. M.; Chen, B. W.; Zhang, J. L.; Xia, G. G.; Hu, J. Z.; Graff, G.; Liu, J.; Yang, Z. G. A Stable Vanadium Redox-Flow Battery with High Energy Density for Large-Scale Energy Storage. *Adv. Energy Mater.* **2011**, *1* (3), 394−400.

(11) Wei, X. L.; Pan, W. X.; Duan, W. T.; Hollas, A.; Yang, Z.; Li, B.; Nie, Z. M.; Liu, J.; Reed, D.; Wang, W.; Sprenkle, V. Materials and Systems for Organic Redox Flow Batteries: Status and Challenges. *ACS Energy Letters* **2017**, *2* (9), 2187−2204.

(12) Kwabi, D. G.; Ji, Y.; Aziz, M. J. Electrolyte lifetime in aqueous organic redox flow batteries: A critical review. *Chem. Rev.* **2020**, *120* (14), 6467−6489.

(13) Brushett, F. R.; Aziz, M. J.; Rodby, K. E. On lifetime and cost of redox-active organics for aqueous flow batteries. *ACS Energy Letters* **2020**, *5*, 879−884.

(14) Huskinson, B. T.; Marshak, M. P.; Suh, C.; Er, S.; Gerhardt, M. R.; Galvin, C. J.; Chen, X.; Aspuru-Guzik, A.; Gordon, R. G.; Aziz, M. J. A metal-free organic-inorganic aqueous flow battery. *Nature* **2014**, *505* (7482), 195−8.

(15) Lin, K.; Chen, Q.; Gerhardt, M. R.; Tong, L.; Kim, S. B.; Eisenach, L.; Valle, A. W.; Hardee, D.; Gordon, R. G.; Aziz, M. J.; Marshak, M. P. Alkaline quinone flow battery. *Science* **2015**, *349* (6255), 1529−32.

(16) Gerhardt, M. R.; Tong, L.; Gomez-Bombarelli, R.; Chen, Q.; Marshak, M. P.; Galvin, C. J.; Aspuru-Guzik, A.; Gordon, R. G.; Aziz, M. J. Anthraquinone Derivatives in Aqueous Flow Batteries. *Adv. Energy Mater.* **2017**, *7* (8), 1601488.

(17) Yang, Z.; Tong, L.; Tabor, D. P.; Beh, E. S.; Goulet, M. A.; De Porcellinis, D.; Aspuru-Guzik, A.; Gordon, R. G.; Aziz, M. J. Alkaline

Benzoquinone Aqueous Flow Battery for Large-Scale Storage of Electrical Energy. *Adv. Energy Mater.* **2018**, *8* (8), 1702056.
(18) Cao, J. Y.; Tao, M.; Chen, H. P.; Xu, J.; Chen, Z. D. A highly reversible anthraquinone-based anolyte for alkaline aqueous redox flow batteries. *J. Power Sources* **2018**, *386*, 40−46.
(19) Kwabi, D. G.; Lin, K.; Ji, Y.; Kerr, E. F.; Goulet, M.-A.; De Porcellinis, D.; Tabor, D. P.; Pollack, D. A.; Aspuru-Guzik, A.; Gordon, R. G.; Aziz, M. J. Alkaline Quinone Flow Battery with Long Lifetime at pH 12. *Joule* **2018**, *2* (9), 1907−1908.
(20) Jin, S.; Jing, Y.; Kwabi, D. G.; Ji, Y.; Tong, L.; De Porcellinis, D.; Goulet, M. A.; Pollack, D. A.; Gordon, R. G.; Aziz, M. J. A water-miscible quinone flow battery with high volumetric capacity and energy density. *ACS Energy Letters* **2019**, *4* (6), 1342−1348.
(21) Park, M.; Beh, E. S.; Fell, E. M.; Jing, Y.; Kerr, E. F.; De Porcellinis, D.; Goulet, M. A.; Ryu, J.; Wong, A. A.; Gordon, R. G.; Cho, J.; Aziz, M. J. A High Voltage Aqueous Zinc-Organic Hybrid Flow Battery. *Adv. Energy Mater.* **2019**, *9* (25), 1900694.
(22) Tong, L.; Goulet, M.-A.; Tabor, D. P.; Kerr, E. F.; De Porcellinis, D.; Fell, E. M.; Aspuru-Guzik, A.; Gordon, R. G.; Aziz, M. J. Molecular Engineering of an Alkaline Naphthoquinone Flow Battery. *ACS Energy Letters* **2019**, *4* (8), 1880−1887.
(23) Hu, B.; Luo, J.; Hu, M.; Yuan, B.; Liu, T. L. A pH-Neutral, Metal-Free Aqueous Organic Redox Flow Battery Employing an Ammonium Anthraquinone Anolyte. *Angew. Chem. Int. Edit* **2019**, *58* (46), 16629−16636.
(24) Ji, Y.; Goulet, M. A.; Pollack, D. A.; Kwabi, D. G.; Jin, S.; Porcellinis, D.; Kerr, E. F.; Gordon, R. G.; Aziz, M. J. A Phosphonate-Functionalized Quinone Redox Flow Battery at Near-Neutral pH with Record Capacity Retention Rate. *Adv. Energy Mater.* **2019**, *9* (12), 1900039.
(25) Wu, M.; Jing, Y.; Wong, A. A.; Fell, E. M.; Jin, S.; Tang, Z.; Gordon, R. G.; Aziz, M. J. Extremely stable anthraquinone negolytes synthesized from common precursors. *Chem-Us* **2020**, *6* (11), 1432−1442.
(26) Jing, Y.; Wu, M.; Wong, A. A.; Fell, E. M.; Jin, S.; Pollack, D. A.; Kerr, E. F.; Gordon, R. G.; Aziz, M. J. In situ electrosynthesis of anthraquinone electrolytes in aqueous flow batteries. *Green Chem.* **2020**, *22* (18), 6084−6092.
(27) Hu, P. F.; Lan, H.; Wang, X.; Yang, Y.; Liu, X. Y.; Wang, H.; Guo, L. Renewable-lawsone-based sustainable and high-voltage aqueous flow battery. *Energy Storage Mater.* **2019**, *19*, 62−68.
(28) Wang, C. X.; Yang, Z.; Wang, Y. R.; Zhao, P. Y.; Yan, W.; Zhu, G. Y.; Ma, L. B.; Yu, B.; Wang, L.; Li, G. G.; Liu, J.; Jin, Z. High-Performance Alkaline Organic Redox Flow Batteries Based on 2-Hydroxy-3-carboxy-1,4-naphthoquinone. *Acs Energy Letters* **2018**, *3* (10), 2404−2409.
(29) Zhu, Y.; Li, Y.; Qian, Y.; Zhang, L.; Ye, J.; Zhang, X.; Zhao, Y. Anthraquinone-based anode material for aqueous redox flow batteries operating in nondemanding atmosphere. *J. Power Sources* **2021**, *501*, 229984.
(30) Aziz, M. J.; Gordon, R. G.; Lin, K.; Kwabi, D. G.; Ji, X. Quinones Having High Capacity Retention For Use Aa Electrolytes In Aqueous Redox Flow Batteries. US2021/0009497 A1, 2021.
(31) Wu, M.; Bahari, M.; Jing, Y.; Amini, K.; Fell, E. M.; George, T. Y.; Gordon, R. G.; Aziz, M. J. Highly Stable Low Redox Potential Quinone for Aqueous Flow Batteries. *Batteries & Supercaps* **2022**, *5*, e202200009.
(32) Jing, Y.; Fell, E. M.; Wu, M.; Jin, S.; Ji, Y.; Pollack, D. A.; Tang, Z.; Ding, D.; Bahari, M.; Goulet, M.-A.; Tsukamoto, T.; Gordon, R. G.; Aziz, M. J. Anthraquinone Flow Battery Reactants with Nonhydrolyzable Water-Solubilizing Chains Introduced via a Generic Cross-Coupling Method. *ACS Energy Letters* **2022**, *7* (1), 226−235.
(33) Wu, M.; Bahari, M.; Fell, E.; Gordon, R. G.; Aziz, M. J. High-Performance Anthraquinone with Potentially Low Cost for Aqueous Redox Flow Batteries. *J. Mater. Chem. A* **2021**, *9*, 26709.
(34) Li, Y.; Xu, Z.; Liu, Y.; Jin, S.; Fell, E. M.; Wang, B.; Gordon, R. G.; Aziz, M. J.; Yang, Z.; Xu, T. Functioning water-insoluble ferrocenes for aqueous organic flow battery via host-guest inclusion. *ChemSusChem* **2021**, *14* (745), 745.
(35) Zhao, Z.; Zhang, B.; Schrage, B. R.; Ziegler, C. J.; Boika, A. Investigations Into Aqueous Redox Flow Batteries Based on Ferrocene Bisulfonate. *ACS Applied Energy Materials* **2020**, *3* (10), 10270−10277.
(36) Yu, J.; Salla, M.; Zhang, H.; Ji, Y.; Zhang, F.; Zhou, M.; Wang, Q. A robust anionic sulfonated ferrocene derivative for pH-neutral aqueous flow battery. *Energy Storage Mater.* **2020**, *29*, 216−222.
(37) Hu, B.; DeBruler, C.; Rhodes, Z.; Liu, T. L. Long-Cycling Aqueous Organic Redox Flow Battery (AORFB) toward Sustainable and Safe Energy Storage. *J. Am. Chem. Soc.* **2017**, *139* (3), 1207−1214.
(38) Beh, E. S.; De Porcellinis, D.; Gracia, R. L.; Xia, K. T.; Gordon, R. G.; Aziz, M. J. A Neutral pH Aqueous Organic-Organometallic Redox Flow Battery with Extremely High Capacity Retention. *ACS Energy Letters* **2017**, *2* (3), 639−644.
(39) Wu, W.; Luo, J.; Wang, F.; Yuan, B.; Liu, T. L. A Self-Trapping, Bipolar Viologen Bromide Electrolyte for Redox Flow Batteries. *ACS Energy Letters* **2021**, *6*, 2891−2897.
(40) Ohira, A.; Funaki, T.; Ishida, E.; Kim, J.-D.; Sato, Y. Redox-Flow Battery Operating in Neutral and Acidic Environments with Multielectron-Transfer-Type Viologen Molecular Assembly. *ACS Applied Energy Materials* **2020**, *3* (5), 4377−4383.
(41) Liu, Y.; Li, Y.; Zuo, P.; Chen, Q.; Tang, G.; Sun, P.; Yang, Z.; Xu, T. Screening Viologen Derivatives for Neutral Aqueous Organic Redox Flow Batteries. *ChemSusChem* **2020**, *13*, 2245.
(42) Jin, S.; Fell, E. M.; Vina-Lopez, L.; Jing, Y.; Michalak, P. W.; Gordon, R. G.; Aziz, M. J. Near Neutral pH Redox Flow Battery with Low Permeability and Long-Lifetime Phosphonated Viologen Active Species. *Adv. Energy Mater.* **2020**, *10* (20), 2000100.
(43) Pang, S.; Wang, X.; Wang, P.; Ji, Y. Biomimetic Amino Acid Functionalized Phenazine Flow Batteries with Long Lifetime at Near-Neutral pH. *Angew. Chem. Int. Edit* **2021**, *60*, 5289−5298.
(44) Xu, J.; Pang, S.; Wang, X.; Wang, P.; Ji, Y. Ultrastable aqueous phenazine flow batteries with high capacity operated at elevated temperatures. *Joule* **2021**, *5* (9), 2437−2449.
(45) Wang, C.; Li, X.; Yu, B.; Wang, Y.; Yang, Z.; Wang, H.; Lin, H.; Ma, J.; Li, G.; Jin, Z. Molecular Design of Fused-Ring Phenazine Derivatives for Long-Cycling Alkaline Redox Flow Batteries. *ACS Energy Letters* **2020**, *5* (2), 411−417.
(46) Hollas, A.; Wei, X. L.; Murugesan, V.; Nie, Z. M.; Li, B.; Reed, D.; Liu, J.; Sprenkle, V.; Wang, W. A biomimetic high-capacity phenazine-based anolyte for aqueous organic redox flow batteries. *Nat. Energy* **2018**, *3* (6), 508−514.
(47) Winsberg, J.; Stolze, C.; Muench, S.; Liedl, F.; Hager, M. D.; Schubert, U. S. TEMPO/Phenazine Combi-Molecule: A Redox-Active Material for Symmetric Aqueous Redox-Flow Batteries. *ACS Energy Letters* **2016**, *1* (5), 976−980.
(48) Lin, K.; Gomez-Bombarelli, R.; Beh, E. S.; Tong, L.; Chen, Q.; Valle, A.; Aspuru-Guzik, A.; Aziz, M. J.; Gordon, R. G. A redox-flow battery with an alloxazine-based organic electrolyte. *Nat. Energy* **2016**, *1* (9), 16102.
(49) Liu, T. B.; Wei, X. L.; Nie, Z. M.; Sprenkle, V.; Wang, W. A Total Organic Aqueous Redox Flow Battery Employing a Low Cost and Sustainable Methyl Viologen Anolyte and 4-HO-TEMPO Catholyte. *Adv. Energy Mater.* **2016**, *6* (3), 1501449.
(50) Janoschka, T.; Morgenstern, S.; Hiller, H.; Friebe, C.; Wolkersdorfer, K.; Haupler, B.; Hager, M. D.; Schubert, U. S. Synthesis and characterization of TEMPO- and viologen-polymers for water-based redox-flow batteries. *Polym. Chem-Uk* **2015**, *6* (45), 7801−7811.
(51) Winsberg, J.; Janoschka, T.; Morgenstern, S.; Hagemann, T.; Muench, S.; Hauffman, G.; Gohy, J. F.; Hager, M. D.; Schubert, U. S. Poly(TEMPO)/Zinc Hybrid-Flow Battery: A Novel, "Green," High Voltage, and Safe Energy Storage System. *Adv. Mater.* **2016**, *28* (11), 2238−43.
(52) Winsberg, J.; Stolze, C.; Schwenke, A.; Muench, S.; Hager, M. D.; Schubert, U. S. Aqueous 2,2,6,6-Tetramethylpiperidine-N-oxyl Catholytes for a High-Capacity and High Current Density Oxygen-

https://doi.org/10.1021/acsenergylett.2c01691
ACS Energy Lett. 2023, 8, 600−607

Insensitive Hybrid-Flow Battery. *ACS Energy Letters* **2017**, *2* (2), 411−416.
(53) Liu, Y. H.; Goulet, M. A.; Tong, L. C.; Liu, Y. Z.; Ji, Y. L.; Wu, L.; Gordon, R. G.; Aziz, M. J.; Yang, Z. J.; Xu, T. W. A Long-Lifetime All-Organic Aqueous Flow Battery Utilizing TMAP-TEMPO Radical. *Chem-Us* **2019**, *5* (7), 1861−1870.
(54) Páez, T.; Martínez-Cuezva, A.; Palma, J.; Ventosa, E. Revisiting the cycling stability of ferrocyanide in alkaline media for redox flow batteries. *J. Power Sources* **2020**, *471*, 228453.
(55) Trant, C.; Vercillo, P. *Solubility of Sodium Ferrocyanide and Potassium Ferrocyanide in Solutions of NaOH and KOH Mixtures at 25°C*; University of Rochester: 2011.
(56) Esswein, A. J.; Goeltz, J.; Amadeo, D. High Solubility Iron Hexacyanides. Application US2014/0051003 A1, 2/20/2014, 2014.
(57) Luo, J.; Hu, B.; Debruler, C.; Bi, Y. J.; Zhao, Y.; Yuan, B.; Hu, M. W.; Wu, W. D.; Liu, T. L. Unprecedented Capacity and Stability of Ammonium Ferrocyanide Catholyte in pH Neutral Aqueous Redox Flow Batteries. *Joule* **2019**, *3* (1), 149−163.
(58) Gregory, T. D.; Perry, M. L.; Albertus, P. Cost and price projections of synthetic active materials for redox flow batteries. *J. Power Sources* **2021**, *499*, 229965.
(59) Kilinkissa, O. E. Y.; Govender, K. K.; Báthori, N. B. Melting point−solubility−structure correlations in chiral and racemic model cocrystals. *CrystEngComm* **2020**, *22* (16), 2766−2771.
(60) Gavezzotti, A.; Rizzato, S. Are Racemic Crystals Favored over Homochiral Crystals by Higher Stability or by Kinetics? Insights from Comparative Studies of Crystalline Stereoisomers. *Journal of Organic Chemistry* **2014**, *79* (11), 4809−4816.
(61) Jing, Y.; Zhao, E. W.; Goulet, M.-A.; Bahari, M.; Fell, E. M.; Jin, S.; Davoodi, A.; Jónsson, E.; Wu, M.; Grey, C. P.; Gordon, R. G.; Aziz, M. J. In situ electrochemical recomposition of decomposed redox-active species in aqueous organic flow batteries. *Nat. Chem.* **2022**, *14* (10), 1103−1109.
(62) Goulet, M.-A.; Tong, L.; Pollack, D. A.; Tabor, D. P.; Odom, S. A.; Aspuru-Guzik, A.; Kwan, E. E.; Gordon, R. G.; Aziz, M. J. Extending the lifetime of organic flow batteries via redox state management. *J. Am. Chem. Soc.* **2019**, *141* (20), 8014−8019.
(63) Kwabi, D. G.; Ji, Y.; Aziz, M. J. Electrolyte lifetime in aqueous organic redox flow batteries: A critical review. *Chem. Rev.* **2020**, *120* (14), 6467−6489.
(64) Luo, J.; Hu, B.; Debruler, C.; Liu, T. L. A pi-Conjugation Extended Viologen as a Two-Electron Storage Anolyte for Total Organic Aqueous Redox Flow Batteries. *Angew. Chem. Int. Edit* **2018**, *57* (1), 231−235.
(65) Hu, B.; Tang, Y.; Luo, J.; Grove, G.; Guo, Y.; Liu, T. L. Improved radical stability of viologen anolytes in aqueous organic redox flow batteries. *Chem. Commun.* **2018**, *54* (50), 6871−6874.
(66) DeBruler, C.; Hu, B.; Moss, J.; Liu, X. A.; Luo, J. A.; Sun, Y. J.; Liu, T. L. Designer Two-Electron Storage Viologen Anolyte Materials for Neutral Aqueous Organic Redox Flow Batteries. *Chem-Us* **2017**, *3* (6), 961−978.
(67) Liu, X.; Zhang, X.; Li, G.; Zhang, S.; Zhang, B.; Ma, W.; Wang, Z.; Zhang, Y.; He, G. Thienoviologen anolytes for aqueous organic redox flow batteries with simultaneously enhanced capacity utilization and capacity retention. *Journal of Materials Chemistry A* **2022**, *10*, 9830−9836.
(68) Liu, B.; Tang, C. W.; Jiang, H.; Guocheng, J.; Zhao, T. An aqueous organic redox flow battery employing a trifunctional electroactive compound as anolyte, catholyte and supporting electrolyte. *J. Power Sources* **2020**, *477*, 228985.
(69) Zhang, S.; Li, X.; Chu, D. D. An Organic Electroactive Material for Flow Batteries. *Electrochim. Acta* **2016**, *190*, 737−743.
(70) Lai, Y. Y.; Li, X.; Liu, K.; Tung, W.-Y.; Cheng, C.-F.; Zhu, Y. Stable Low-Cost Organic Dye Anolyte for Aqueous Organic Redox Flow Battery. *ACS Applied Energy Materials* **2020**, *3* (3), 2290−2295.
(71) Huang, J. H.; Yang, Z.; Murugesan, V.; Walter, E.; Hollas, A.; Pan, B. F.; Assary, R. S.; Shkrob, I. A.; Wei, X. L.; Zhang, Z. C. Spatially Constrained Organic Diquat Anolyte for Stable Aqueous Flow Batteries. *Acs Energy Letters* **2018**, *3* (10), 2533−2538.
(72) Sun, P.; Liu, Y. H.; Li, Y. Y.; Shehzad, M. A.; Liu, Y. Z.; Zuo, P. P.; Chen, Q. R.; Yang, Z. J.; Xu, T. W. 110th Anniversary: Unleashing the Full Potential of Quinones for High Performance Aqueous Organic Flow Battery. *Ind. Eng. Chem. Res.* **2019**, *58* (10), 3994−3999.
(73) Orita, A.; Verde, M. G.; Sakai, M.; Meng, Y. S. A biomimetic redox flow battery based on flavin mononucleotide. *Nat. Commun.* **2016**, *7*, 13230.
(74) Janoschka, T.; Martin, N.; Hager, M. D.; Schubert, U. S. An Aqueous Redox-Flow Battery with High Capacity and Power: The TEMPTMA/MV System. *Angew. Chem., Int. Ed. Engl.* **2016**, *55* (46), 14427−14430.
(75) Liu, Y. Y.; Lu, S. F.; Chen, S.; Wang, H. N.; Zhang, J.; Xiang, Y. A Sustainable Redox Flow Battery with Alizarin-Based Aqueous Organic Electrolyte. *Acs Applied Energy Materials* **2019**, *2* (4), 2469−2474.
(76) Luo, J.; Wu, W. D.; Debruler, C.; Hu, B.; Hu, M. W.; Liu, T. L. A 1.51 V pH neutral redox flow battery towards scalable energy storage. *J. Mater. Chem. A* **2019**, *7* (15), 9130−9136.
(77) Xia, L.; Zhang, F.; Wang, F.; Chu, F.; Yang, Y.; Li, H.; Tan, Z. A Low-Potential and Stable Bis-Dimethylamino Substituted Anthraquinone for pH-Neutral Aqueous Redox Flow Batteries. *ChemElectroChem.* **2022**, *9*, e202200224.
(78) Chen, Q.; Li, Y.; Liu, Y.; Sun, P.; Yang, Z.; Xu, T. Designer Ferrocene Catholyte for Aqueous Organic Flow Batteries. *ChemSusChem* **2021**, *14*, 1295.
(79) Feng, R.; Murugesan, V.; Hollas, A.; Chen, Y.; Shao, Y.; Walter, E.; Wellala, N.; Yan, L.; Rosso, K. M.; Wang, W.; Zhang, X. Reversible ketone hydrogenation and dehydrogenation for aqueous organic redox flow batteries. *Science* **2021**, *372*, 836.
(80) Tang, G.; Liu, Y.; Li, Y.; Peng, K.; Zuo, P.; Yang, Z.; Xu, T. Designing Robust Two-Electron Storage Extended Bipyridinium Anolytes for pH-Neutral Aqueous Organic Redox Flow Batteries. *JACS Au* **2022**, *2* (5), 1214−1222.
(81) Guiheneuf, S.; Godet-Bar, T.; Fontmorin, J.-M.; Jourdin, C.; Floner, D.; Geneste, F. A new hydroxyanthraquinone derivative with a low and reversible capacity fading process as negolyte in alkaline aqueous redox flow batteries. *J. Power Sources* **2022**, *539*, 231600.
(82) Wang, X.; Wang, P. H. P.; Cao, Y.; Mercier, P. P. A 0.6V 75nW All-CMOS Temperature Sensor With 1.67m°C/mV Supply Sensitivity. *IEEE Transactions on Circuits and Systems I: Regular Papers* **2017**, *64* (9), 2274−2283.

https://doi.org/10.1021/acsenergylett.2c01691
ACS Energy Lett. 2023, 8, 600−607